БЪЛГАРСКА АКАДЕМИЯ НА НАУКИТЕ BULGARIAN ACADEMY OF SCIENCES
ТЕОРЕТИЧНА И ПРИЛОЖНА МЕХАНИКА THEORETICAL AND APPLIED MECHANICS
София, 1989, год. XX, № 3 Sofia, 1989, Year XX, No 3

Механика на флуидите

Quasi one-dimensional model of drawing of glass microcapillaries and approximate solutions

A. Yarin, Vl. Rusinov, P. Gospodinov, St. Radev

The mathematical models of drawing of glass microcapillaries and fibres, using cylindrical rods, are discussed in [1] and [2]. There one-dimensional equations are obtained on the basis of Navier-Stokes equations and the thermal conductivity equation. However, a cylindrical axi-symmetric coordinate system is employed and the curvature effects are taken into account in the boundary conditions at the fibre surface.

To study the spatial flow of thin capillary jets, quasi one-dimensional equations are derived in [3] and [4] by introducing a local coordinate system attached to the jet axis. The present paper proposes a quasi one-dimensional model in order to describe the steady drawing of microcapillaries by using preform glass tubes which are heated in cylindrical furnaces. An approximate nonisothermal analytical solution, as well as a simplified numerical solution, are obtained by disregarding the surface and gravity forces. The results from the numerical solution and a comparison between the numerical and the nonisothermal analytical solution are presented graphically.

1. Quasi one-dimensional model

The process is shown schematically in Fig. 1, where x denotes the longitudinal coordinate along the symmetry axis which varies from 0 to L (here L is the furnace length).

The glass tube enters the furnace (where $x=0$) with velocity V_0 and temperature T_0. R_0 and h_0 are the average radius and the average thickness of the tube wall respectively. The glass microcapillary, with dimensions R_1, h_1 and temperature T_1, is drawn at the furnace exit (there $x=L$).

The Navier-Stokes equations, together with the heat conductivity equation, are solved by employing a moving coordinate system, with unit vectors $\vec{\tau}$, $\vec{n}$ and $\vec{b}$ along the tangent, the normal and the binormal respectively. Assuming that the gradients of the tangential velocity and temperature along n are zero, as well as that the normal cross-sections remain plane, the following quasi one-dimensional steady model is obtained

(1) $$RhV=Q,$$

(2) $$\rho Q\frac{dV}{dx}=\frac{d}{dx}(\Sigma_{\tau\tau}Rh)-\Sigma_{\Theta\Theta}h\frac{dR}{dx}+\rho ghR,$$

(3) $$\rho Q V\lambda k=\Sigma_{\tau\tau}Rh\lambda k-\Sigma_{\Theta\Theta}h+2\sigma(R\lambda k-1)-\rho ghR\,\frac{dR}{dx},$$

(4) $$\rho c_p Q\frac{dT}{dx}=-(q_{n,1}+q_{n,2})\,\lambda R,$$

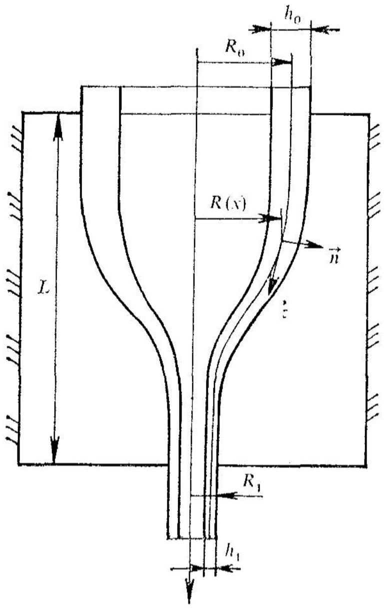

Fig. 1

where the approach given in [3], [4] and [5] has been adopted. The normal components of the stress tensor along the tangent and the binormal are given by

(5) $$\Sigma_{\tau\tau}=2\mu\left(\frac{2}{\lambda}\,\frac{dV}{dx}+\frac{V}{\lambda R}\,\frac{dR}{dx}\right),$$

(6) $$\Sigma_{\Theta\Theta}=2\mu\left(\frac{1}{\lambda}\,\frac{dV}{dx}+\frac{2V}{\lambda R}\,\frac{dR}{dx}\right).$$

The softened glass is considered to be a Newtonian fluid, with viscosity μ depending on the temperature, i. e. $\mu=\mu(T)$. The following notations are used in Eqns (1)—(6):

Q — volume output; ρ — glass density; g — gravity acceleration; c_p — isobaric heat capacity; σ — surface tension coefficient. Here, applying Frenet's formulas as in [3] and [4], the arc length of the curve, obtained as a section of the middle surface with the axial plane, is used as a parameter, so

(7) $$\lambda=\sqrt{1+\left(\frac{dR}{dx}\right)^2},$$

(8) $$k=\frac{d^2R}{dx^2}\,\lambda^{-3},$$

with λ and k being the Lame coefficient and the curvature.

Equations (1)—(8) differ from these obtained in [1] because here is included the nonzero component of the stress tensor along the binormal $\vec{b}$ and the curvature due the action of the surface forces and gravity is taken into account. Hence, the obtained quasi one-dimensional model is more complete.

The effects of λ and k, of order higher than that of the values given in (1)—(6), are neglected. $q_{n,2}$ and $q_{n,1}$ denote the thermal fluxes along the inside and the outside normal, directed towards the middle surface. From now on $q_{n,2}$ will be disregarded.

The complex character of the model (1)—(6) does not allow for a solution of a closed form. The analytical solutions can be obtained for some special cases only, by simplifying the obtained model. The action of inertia and gravity forces, as well as that of the surface tension, can be disregarded as insignificant. The same is with the effects which account for curvature and slope of the average surface, i. e. $k=0$; $\lambda=1$. These long-wave assumptions lead to the statesment that the viscous stresses along the tangent $\Sigma_{\tau\tau}$ prevail over the viscous stresses along the binormal $\Sigma_{\Theta\Theta}$ ($\Sigma_{\Theta\Theta}=0$), and hence to

(9) $$\frac{dV}{dx}+\frac{2V}{R}\,\frac{dR}{dx}=0.$$

On the other hand, the assumption that the glass viscosity does not depend on the fibre temperature makes possible an additional simplification of the model by excluding Eqn (4).

The direct integration of the system thus simplified, obtained from (1) — (6), yields

$$V(x)=V_0E^{\frac{x}{L}}, \tag{10}$$

$$R(x)=R_0\,E^{-\frac{x}{2L}}, \tag{11}$$

$$h(x)=h_0E^{-\frac{x}{2L}}, \tag{12}$$

where $E=V_1/V_0$ is the draw ratio.

2. Nonisothermal analytical solution

The nonisothermal analytical solution which gives a relation between the geometric and kinematic characteristics of the process, on the one hand, and the longitudinal coordinate x, on the other, is obtained by using the Arrhenius' temperature relation for the material viscosity:

$$\mu=\mu_0\,.\exp\left(\frac{U}{GT}\right), \tag{13}$$

where μ_0 is a constant quantity, U is the activation energy and G is the gas constant.

The essential supposition when deriving this solution is that the activation energy U is sufficient enough, which allows to integrate the equations in a vicinity of a point where the temperature profile attains its maximum $T=T_p$ (for $x=l$). Such an approach is used in [6], but for a compact fibre.

The nonisothermal analytical solution has the form:

— in the heating region $(T_0\leq T(x)\leq T_p)$

$$\bar{R}=\bar{h}=1-(1-m)\,.\exp\left[\Theta(\bar{T}-1)\right], \tag{14}$$

$$\bar{x}=-\frac{T_p\cdot\rho\,.\,c_p\,.\,Q}{L\,.\,q_1\,.\,R_0}\{\bar{T}-\bar{T}_0-\Theta^{-1}\,.\ln\left[1-(1-m)\,.\exp\left[\Theta(\bar{T}-1)\right]\right]\}; \tag{15}$$

— in the cooling region $(T_p\geq T(x)\geq T_1)$

$$\bar{R}=\bar{h}=m-(E^{-\frac{1}{2}}-m)\{\exp\left[\Theta(\bar{T}-1)\right]-1\}, \tag{16}$$

$$\bar{x}=\frac{l}{L}-\frac{T_p\cdot\rho\,.\,c_p\,.\,Q}{L\,.\,q_1\,.\,R_0}\,E^{\frac{1}{2}}\left(\frac{q_2}{q_1}\right)^{-1} \tag{17}$$

$$\times\left\{\bar{T}-1-\Theta^{-1}\,.\ln\left[m^{-1}E^{-\frac{1}{2}}-(m^{-1}E^{-\frac{1}{2}}-1)\,.\exp\left[\Theta(\bar{T}-1)\right]\right]\right\}.$$

The velocity in both regions is expressed by:

$$\bar{V}=\bar{R}^{-2}, \tag{18}$$

where m is given by

$$m=\frac{1-E^{-\frac{1}{2}}\cdot\left(\frac{q_2}{q_1}\right)}{1-\left(\frac{q_2}{q_1}\right)}. \tag{19}$$

The following notations are used in Eqns (14)—(19): $\bar{R}=\frac{R(x)}{R_0}$ — dimensionless average radius; $\bar{h}=\frac{h(x)}{h_0}$ — dimensionless thickness; $\bar{V}=\frac{V(x)}{V_0}$ — dimensionless velocity; $\bar{T}=\frac{T(x)}{T_p}$ — dimensionless temperature. q_2 and q_1 denote fluxes of cooling and heating of tube in the furnace and outside it.

The maximum temperature and the relation between T_1 and L are given oy

$$T_P=\frac{U}{2.G.\ln(m)}+\left[\frac{U^2}{4.G^2\ln^2(m)}-\frac{U}{G.\ln(m)}\left(T_0-l\frac{q_1R_0}{\rho c_pQ}\right)\right]^{\frac{1}{2}}, \tag{20}$$

$$T_1=T_P.\left[1-\Theta^{-1}\ln(m^{-11}E^{-1/2})-\frac{(L-l)\,R_0\,q_2}{E^{1/2}\,T_p.\rho.c_p.Q}\right],$$

where l is the value of the coordinate x for which $T=T_P$. It is expressed as follows

$$l=-\frac{T_p.\rho.c_p.Q}{q_1.R_0}\left(1-\frac{T_0}{T_p}-\Theta^{-1}\ln(m)\right);\quad \Theta=\frac{U}{G.T_p}. \tag{21}$$

3. Simplified numerical solution

The restrictions imposed on the construction of the analytical solution induce certain difficulties when modelling the drawing process.

To account for the action of surface and gravity forces, for the real conditions of heat exchange, as well as for curvature effects, we must solve the initial quasi one-dimensional model numerically. The ordinary differential equations in the system (1)—(6) require the choice of an appropriate numerical scheme for their solution, combined with an iteration procedure.

Looking for a numerical solution, some difficulties arise, due to the singularities in the higher derivative terms of the system (1)—(8). The first step to such a solution is to regard some of the assumptions under which the analytical, nonisothermal solution was obtained. This enables us, when analysing the terms of Equation (3), to consider the term with $\Sigma_{\Theta\Theta}$ as a principal one, while the rest of the terms, containing k, σ or g are of an order less than $\Sigma_{\Theta\Theta}$. Then it can be assumed, as a first approximation, that $\Sigma_{\Theta\Theta}=0$.

When solving the initial model, the following viscosity — temperature relation is used:

$$\mu=10^{\frac{B}{T-T_H}+A}, \tag{22}$$

where A, B and T_H are experimentally determined constants and T is the temperature along x, in ^0K.

The coefficient λ which accounts for the slope of the middle surface remains in Eqns (2) and (4). Unlike the analytical solution, Eqn (2) regards the action of inertia and gravity forces. The energy flux along the normal towards the outside surface of the capillary is given in the thermal conductivity equation as a sum of a convective and radiation flux:

$$q_{n,1}=q_k+q_r \tag{23}$$

where the energy transfer due to convection is expressed by using the relation given in [7]:

$$q_k=\beta(x)\,[T(x)-T_g] \tag{24}$$

with the heat transfer coefficient β in the form:

$$\beta(x)=1{,}982.10^{-4}\,[\pi R^2(x)]^{-\frac{1}{3}}.V^{-\frac{1}{3}}(x). \tag{25}$$

The energy transfer due to radiation is given by

$$q_r=\varkappa.\varepsilon[T^4(x)-T_f^4(x)]. \tag{26}$$

The notations used here are as follows: T_g — the gas temperature ; $\varkappa$ — the Stefan-Boltzmann constant; ε — a reduced degree of blackness of the product-furnace system; $T_f(x)$ — a temperature profile of the furnace wall.

The model equations are given in a dimensionless form for convenience and the kinematic and geometric characteristics V_0 and R_0, h_0 at the furnace entrance ($x=0$) are used as characteristic scales for velocity and length, while the maximum value of $T_f(x)$, (T_{max}) is used as a characteristic scale for temperature. All notations, reduced to a dimensionless form, are kept the same. The following characteristic parameters are included in the dimensionless equations and boundary conditions: $Re=\rho V_0 R_0/\mu_0$ — the Reynolds number; $Fr=V_0^2/gR_0$ — the Froude number; $Bo=\rho.c_p.V_0/\varkappa T_{max}^3$ — the Boltzmann number. μ_0 denotes the chosen viscosity characteristic value (here $\mu_0=10^4$, $\bar{R}=R(x)/R_0$, $\bar{h}=h(x)/h_0$, $\bar{L}=L/R_0$).

The Nusselt number, given by $Nu(x)=\dfrac{\beta(x)}{\rho.c_p.V_0}$, appears in the dimensionless equation of heat transfer.

To solve numerically the dimensionless equations we employ the Runge-Kutta method, where the initial system is written in the form:

$$y_1'=-\frac{y_1 y_5}{2y_3}, \tag{27}$$

$$y_2'=-\frac{y_2 y_5}{2y_3}, \tag{28}$$

$$y_3'=y_5, \tag{29}$$

$$y_4'=\lambda\left[Nu.(\bar{T}_g-y_4)+\varepsilon.(T_f^4-y_4^4)\,\overline{Bo}^{-1}\right]\frac{1}{y_2\,y_3}, \tag{30}$$

$$y_5'=\frac{\lambda}{4\bar{\mu}}Re\left(y_3 y_5-\frac{1}{Fr}\right)+\frac{3}{4}\ln 10.\frac{B}{T_{max}}.\frac{y_4' y_5}{(y_4-\bar{T}_H)^2}+\frac{7}{8}\frac{y_5^2}{y_3}. \tag{31}$$

Here y_i ($i=1, 2 \dots 5$) denote respectively: $y_1=\bar{R}(\bar{x})$, $y_2=\bar{h}(\bar{x})$, $y_3=\bar{V}(\bar{x})$, $y_4=\bar{T}(\bar{x})$, $y_5=d\bar{V}/d\bar{x}$, and $\bar{\mu}=\mu/\mu_0$.

The following initial and boundary conditions are used: $\bar{R}_0=1$, $\bar{h}_0=0{,}185$, $\bar{T}_0=0{,}230$, $\bar{V}_0=1$, $V_1=1{,}7.10^3$. The dimensionless temperature profile $\bar{T}_f(\bar{x})$ of the furnace is included in the system. Depending on the furnace length, it is given as follows:

— for $0\leq\bar{x}\leq\bar{L}_1$, $\bar{T}_f=\bar{T}_{f,1}+\dfrac{1-\bar{T}_{f,1}}{\bar{L}_1}.\bar{x}$,

— for $\bar{L}_1 \le \bar{x} \le \bar{L}_2$, $\bar{T}_f = 1$,

— for $\bar{L}_2 \le \bar{x} \le \bar{L}$, $\bar{T}_f = 1 - \dfrac{1-\bar{T}_{f,2}}{\bar{L}-\bar{L}_2}(\bar{x}-\bar{L}_2)$.

The dimensionless temperatures at the furnace entrance and exit are given by $\bar{T}_{f,1}=0{,}29$ and $\bar{T}_{f,2}=0{,}29$ where $\bar{L}_1=0{,}44\,\bar{L}$ and $\bar{L}_2=0{,}55\,\bar{L}$.

A similar profile for the dimensionless temperature $\bar{T}_g$ is introduced, i. e.

— for $0 \le \bar{x} \le \bar{L}_3$, $\bar{T}_g = \bar{T}_{g,1} + \dfrac{1-\bar{T}_{g,1}}{\bar{L}_1}\bar{x}$,

— for $\bar{L}_3 \le \bar{x} \le \bar{L}_4$, $\bar{T}_g = 1$,

— for $\bar{L}_4 \le \bar{x} \le \bar{L}$, $\bar{T}_g = 1 - \dfrac{1-\bar{T}_{g,2}}{\bar{L}-\bar{L}_4}(\bar{x}-\bar{L}_4)$.

The dimensionless temperature of the gas medium, at the furnace entrance and exit respectively, are denoted by $\bar{T}_{g,1}=0{,}615$ and $\bar{T}_{g,2}=0{,}615$, where $\bar{L}_3=\dfrac{\bar{L}}{3}$ and $\bar{L}_4=\dfrac{2\bar{L}}{3}$.

The assumed temperature profiles are close to the real ones.

In order to close the system (27) — (31) we need an extra condition. This is most often the drawing velocity $\bar{V}_1$ for $\bar{x}=\bar{L}$. This leads to a boundary value problem with conditions at both ends of the integration interval and hence, an iteration procedure is to be employed. It has to be organized efficiently so that the boundary condition for $\bar{x}=\bar{L}$ be satisfied with sufficient accuracy, after an appropriate choice of the missing boundary condition.

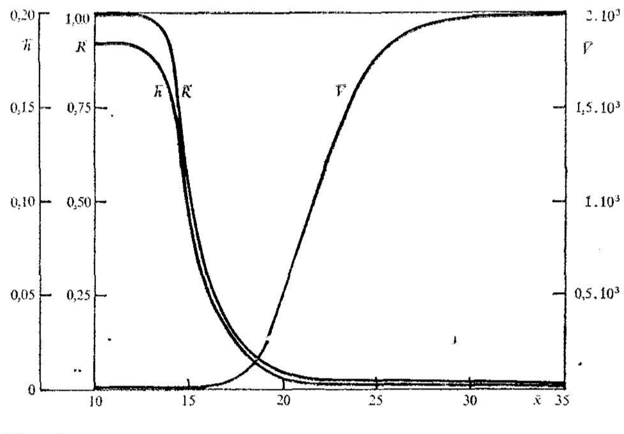

Fig. 2

The variation of the dimensionless radius, thickness and fibre velocity, as a function of the longitudinal coordinate $\bar{x}$, is given in Fig. 2. The results are obtained for $Re=1{,}049\,.\,10^{-4}$, $Fr=4{,}179.\,10^{-8}$, $Bo=1{,}4106$, $\varepsilon=0{,}8$, $\rho=3000$ kg/m^3, $c_p=1000$ $J/kg.deg$.

A comparison of the numerical solution with the analytical nonisothermal solution is given in Fig. 3.

The analytical solution is obtained for a given maximum temperature — $T_P=1300°K$. Then the corresponding length $x=l$ in the heating region is determined according to formula (21). The initial data are as follows: $T_0=300°K$ initial temperature; $\rho=2200$ kg/m³ — material density; $c_P=1043\frac{J}{kg.deg}$ — isobaric heat capacity;

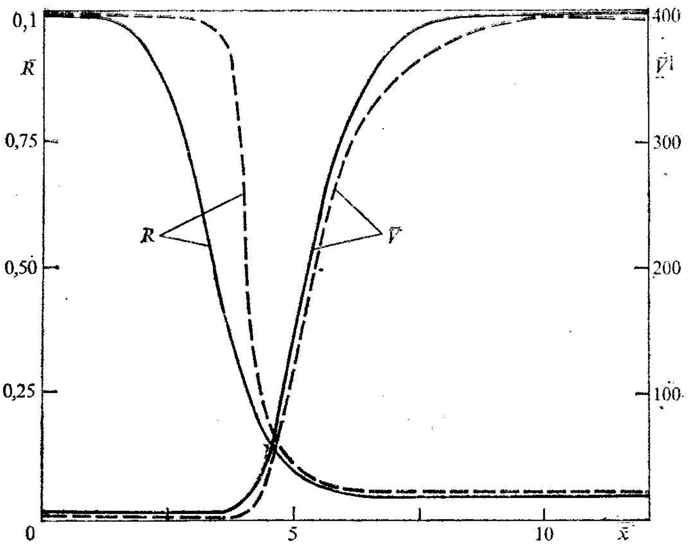

Fig. 3

$q_1=-0{,}465$ wt/m^2 — heating flux; $R_0=0{,}01$ m, $h_0=0{,}001$ m — initial dimensions; $L=1{,}4$ m — furnace length; $E=400$ — drawing rate frequency; $q_2/q_1=-3$.

The same geometrical, physical and thermophysical material characteristics are used for the numerical solution. Here instead of the drawing rate velocity are given $\bar{V}_0=1$ and $\bar{V}_1=400$. The furnace temperature profile $\bar{T}_f(\bar{x})$ and the gas temperature profile $\bar{T}_g(\bar{x})$ are determined after performing numerical experiments, and appropriate values of the temperatures $\bar{T}_{f,1}$ and $\bar{T}_{g,1}$ are sought, while the rest of the parameters remain the same.

Hence, the requirement that the fibre maximum temperature be equal to T_P is satisfied. Moreover, this temperature is be attained for the same length $x=l$, while retaining the heating and cooling intensity. Hence, the following relations $\bar{T}_f(\bar{x})$ and $\bar{T}_g(\bar{x})$ are obtained:

$$\bar{T}_{f,1}=0{,}615;\quad \bar{L}_1=\bar{L}_2=\bar{l};\quad \bar{T}_{f,2}=0{,}230;$$

$$\bar{T}_{g,1}=0{,}615;\quad \bar{L}_3=\bar{L}_4=\bar{l};\quad \bar{T}_{g,2}=0{,}270.$$

The constants A, B and T_H in relation (22) are determined on the basis of three characteristic points of relation (13) and have the following values: $A=1{,}768$, $B=1046{,}8$, $T_H=665{,}7$.

The dense line expresses relations $\bar{R}(\bar{x})$ and $\bar{V}(\bar{x})$ obtained by means of the numerical solution and dash line expresses the analytical one.

Comparing the results of the analytical and the numerical solution for some characteristic cases (short region of intensitive heating, of order of 2-3 times the average radius of the preform, and abrupt cooling after reaching the maximum temperature T_P), it is observed that the heating region length and the temperature gradient dT/dx are significant for the capillars drawing.

The variation of the cooling intensity (q_2/q_1 ratio) does not affect significantly the shape and dimensions of the capillary, but affects only the temperature T_1 at the furnace exit. Thus can be explained the fact that the numerical and analytical results coincide better at the end of the product transition region, as shown in Fig. 3.

4. Conclusions

The complexity of the proposed nonisothermal model is verified by the necessity to reveal the character of the real process. Hence, we have to look for approximate solutions.

The analytical nonisothermal solution is obtained by introducing more simplifications as compared to the construction of the approximate solution. The results given in Fig. 2 show that the numerical solution gives the basic characteristics of the drawing process. The analytical nonisothermal solution (Fig. 3) enables to describe the drawing process with sufficient accuracy when a comparatively short heating region is considered, i. e. when more rapid change of the fibre shape and velocity occurs. Some difference between the analytical and the numerical results at the beginning of the transition region ($1 \leq \bar{x} \leq 4$).

Unlike the numerical solution, a direct relation between T_p and l exists in the analytical solution (Equations (20) and (21)) and abrupt change of the thermal flux at point ($T(x) = T_P$) is assumed. The use of a numerical method implies restrictions on the maximum value of the gradient $\frac{dT}{dx}$, in the heating region. This leads to restrictions on the value of the heating flux $q_{n,1}$ (in (23)) and does not allow to reproduce entirely in the numerical method the heating conditions, employed in the analytical solution. More reliable results can be obtained by a numerical treatment of the full model. Then the approximate solution can be used as an initial approximation.

The comparison of the proposed solution with the solution of the full model is an object of further research.

References

1. Zhabotinskiy, M. E., A. V. Foygel. — Jurn. Prikl. Mech. Teoret. Fiz., 1976, No 2 (Russian).
2. Paek, U. C., R. B. Runk. — Jurn. Appl. Phys., 1978, No 49.
3. Entov, V. M., A. L. Yarin. — Jurn. Fl. Mech., 1984, Vol. 140.
4. Yarin, A. L. — Meh. Zhid. Gasa, 1983, No 1.
5. Entov, V. M., H. S. Kestenboym, A. N. Rozhkov, L. I. Sharchevich. — Mech. Zhid. Gasa, 1980, No 2.
6. Yarin, A. L. — Zh. Prikl. Mech. Teor. Fiz., 1982, No 6.
7. Kase, S., T. Matsuo. — Jurn. App. Pol. Sc., 1967, Vol. 11.

Received 15. 01. 1988